



SoulX-FlashTalk: Real-Time Infinite Streaming of Audio-Driven Avatars via Self-Correcting Bidirectional Distillation

Le Shen^{1,2,‡,*}, Qian Qiao^{1,*}, Tan Yu^{1,*}, Ke Zhou¹,
Tianhang Yu¹, Yu Zhan¹, Zhenjie Wang², Dingcheng Zhen¹, Ming Tao¹, Shunshun Yin¹, Siyuan Liu[†]

¹AIGC Team, Soul AI Lab, China ²Donghua University

Project Page: <https://soul-ailab.github.io/soulx-flashtalk/>

ABSTRACT

Deploying massive diffusion models for real-time, infinite-duration, audio-driven avatar generation presents a significant engineering challenge, primarily due to the conflict between computational load and strict latency constraints. Existing approaches often compromise visual fidelity by enforcing strictly unidirectional attention mechanisms or reducing model capacity. To address this problem, we introduce **SoulX-FlashTalk**, a 14B-parameter framework optimized for high-fidelity real-time streaming. Diverging from conventional unidirectional paradigms, we use a **Self-correcting Bidirectional Distillation** strategy that retains bidirectional attention within video chunks. This design preserves critical spatiotemporal correlations, significantly enhancing motion coherence and visual detail. To ensure stability during infinite generation, we incorporate a **Multi-step Retrospective Self-Correction Mechanism**, enabling the model to autonomously recover from accumulated errors and preventing collapse. Furthermore, we engineered a full-stack inference acceleration suite incorporating hybrid sequence parallelism, Parallel VAE, and kernel-level optimizations. Extensive evaluations confirm that SoulX-FlashTalk is the first 14B-scale system to achieve a **sub-second start-up latency (0.87s)** while reaching a real-time throughput of **32 FPS**, setting a new standard for high-fidelity interactive digital human synthesis.

1 Introduction

Diffusion Transformers (DiTs) [Peebles and Xie, 2023] serve as a scalable backbone for high-fidelity generative modeling. Building on this capability, recent large-scale models [Gao et al., 2025, Zhong et al., 2025, Guo et al., 2024, Yang et al., 2025] have significantly advanced avatar generation, delivering cinematic quality, detailed micro-expressions, and natural full-body dynamics. However, deploying these models for real-time, infinite streaming remains a major engineering challenge. The primary conflict lies between the high computational cost required for high-fidelity generation and the strict low-latency demands of live streaming.

To achieve real-time performance, state-of-the-art approaches like LiveAvatar [Huang et al., 2025a] typically employ a *bidirectional-teacher to unidirectional-student* distillation strategy, combined with multi-GPU parallel inference. While effective, this design requires a complex two-stage training pipeline comprising diffusion forcing and DMD [Yin et al., 2024] distillation. This process is computationally expensive and can require up to 27,500 training steps. More critically, converting the student model to a strictly unidirectional architecture disrupts the spatiotemporal correlations inherent in video generation. This structural mismatch often results in rigid full-body dynamics and a loss of textural detail. Although methods like Self-Forcing [Huang et al., 2025b] and Self-Forcing++ [Cui et al., 2025] simulate autoregressive inference to mitigate error accumulation, applying these mechanisms effectively to a large-scale model under real-time constraints lacks a mature reference solution.

To address these challenges, we introduce **SoulX-FlashTalk**, a low-latency, real-time, audio-driven avatar framework built upon a 14B-parameter DiT. Compared with prior approaches, our method offers substantial advantages across model architecture design, training and distillation strategy, and inference-time optimization, enabling high-fidelity avatar generation while meeting the stringent latency requirements of live streaming.

*Equal contribution. [‡]Work done during an internship at Soul AI Lab. le.shen@mail.dhu.edu.cn, {qiaoqian,yutan}@soulapp.cn

[†]Corresponding authors. liusiyuan@soulapp.cn

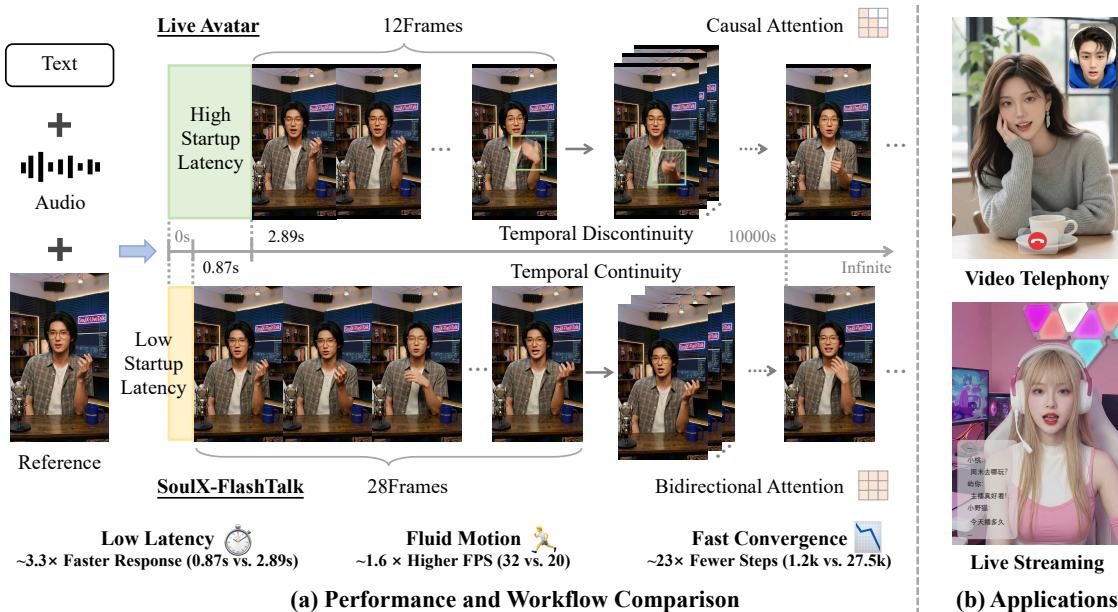


Figure 1: Performance Overview and Applications of SoulX-FlashTalk. (a) Performance and Workflow Comparison: Powered by our bidirectional streaming distillation, SoulX-FlashTalk converges in just 1.2k steps (reducing training costs by $\sim 23\times$ compared to LiveAvatar), achieves a 0.87s start-up latency ($\sim 3.3\times$ faster), and attains fluid motion at 32FPS ($\sim 1.6\times$ higher). (b) Applications: Supports real-time interactions, including Video Telephony and Live Streaming.

First, regarding model architecture and generation quality, we diverge from the strictly unidirectional paradigm by adopting a *bidirectional-teacher to bidirectional-student* strategy. We argue that in chunk-based streaming inference, future information *within* the current chunk is available. Therefore, retaining the bidirectional attention mechanism for intra-chunk processing is not only feasible but beneficial. This design allows the student model to leverage local context for motion planning, significantly enhancing full-body coherence and detail. Crucially, maintaining high architectural alignment between the teacher and student simplifies the distillation task, avoiding the performance degradation caused by structural forcing.

Second, in terms of training efficiency, SoulX-FlashTalk streamlines the time-consuming training paradigm of LiveAvatar [Huang et al., 2025a]. This improvement is enabled by the architectural consistency described above, which allows us to adopt a lightweight yet effective training strategy. **Latency-Aware Spatiotemporal Adaptation** adapts the model to operate effectively under lower spatial resolutions and shorter temporal horizons for real-time constraints. **Self-Correcting Bidirectional Distillation** further reduces inference steps and eliminates classifier-free guidance, while introducing a multi-step retrospective self-correction mechanism inspired by Self-Forcing++ to enable the model to recover from self-induced deviations and prevents collapse during long-horizon generation.

Finally, to meet strict real-time streaming requirements with a large-scale DiTs, we construct a full-stack inference acceleration solution. By utilizing xDiT’s hybrid sequence parallelism (integrating Ulysses [Jacobs et al., 2023] and Ring Attention [Liu et al., 2023]), we achieve an approximate $5\times$ speedup for single-step inference on an 8 GPUs setup. We also address the 3D VAE bottleneck by introducing the slicing parallel strategy from LightX2V [Contributors, 2025], accelerating encoding/decoding by nearly $5\times$. Furthermore, we tailor our kernel implementations for the Hopper architecture to fully exploit its hardware capabilities by adopting FlashAttention3 [Shah et al., 2024]. Combined with `torch.compile` optimizations, these measures maximize hardware utilization.

As shown in Figure 1(a), our model converges to superior performance with only 200 distillation steps, yielding an efficiency improvement of approximately $23\times$ over LiveAvatar, which requires 27,500 steps. Meanwhile, the proposed system achieves a start-up latency of 0.87 s, about $3\times$ faster than prior baselines at 2.89 s. Together with these gains, this report presents comprehensive ablation studies of the proposed optimizations, providing practical guidance for the stable training and real-time deployment of large-scale DiTs.

2 SoulX-FlashTalk

This section details the core methodology of SoulX-FlashTalk. As illustrated in Figure 2, our framework is built upon a 14B-parameter DiT and integrates a two-stage training pipeline with a full-stack inference acceleration engine. The

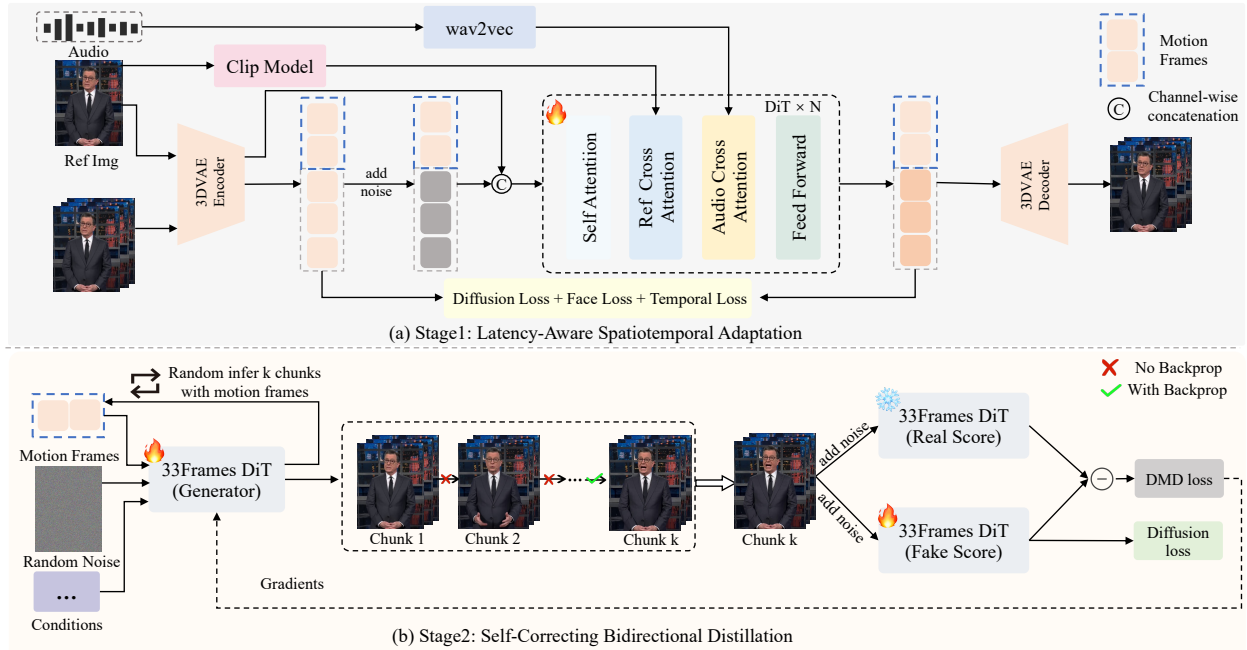


Figure 2: **Framework Overview.** (a) Stage 1: Latency-Aware Spatiotemporal Adaptation, which adapts the model to operate effectively under lower spatial resolutions and shorter temporal frames to meet real-time constraints. (b) Stage 2: Self-Correcting Bidirectional Distillation, where the generator autoregressively synthesizes k chunks conditioned on past motion frames, while the Real and Fake Score networks align data distributions through distillation losses.

training protocol progresses from Latency-Aware Spatiotemporal Adaptation phase to a Self-Correcting Bidirectional Distillation phase, designed to satisfy both high-fidelity generation and low-latency streaming requirements.

2.1 Model Architecture

The architecture derives from WAN2.1-I2V-14B [Wan et al., 2025] and InfiniteTalk [Yang et al., 2025], comprising four primary components:

3D VAE. We utilize the WAN2.1 VAE for latent space compression to facilitate efficient high-resolution video generation. This module encodes video frames into compact latent representations, achieving a spatio-temporal downsampling factor of $4 \times 8 \times 8$ across temporal, height, and width dimensions.

DiT-Based Generator. The core generator adopts the DiT architecture [Peebles and Xie, 2023]. As shown in Figure 2(a), each DiT block incorporates a 3D Attention mechanism to model spatio-temporal dependencies. A unified cross-attention layer conditions the generation on reference images and textual inputs to preserve visual fidelity and provide semantic guidance. Furthermore, we integrate a dedicated audio cross-attention layer to inject speech-driven signals directly into the generation process.

Conditioning Encoders. The model conditions generation on audio, text, and reference images. We employ a Wav2Vec model [Baevski et al., 2020] customized for Chinese speech to transform continuous audio signals into sequential embeddings. To ensure identity consistency, we extract semantic representations and visual features f_{ref} from the reference image using CLIP [Radford et al., 2021] and the VAE encoder. For textual conditioning, we adopt umT5 [Raffel et al., 2020] to support bilingual captions. These identity and textual conditions are injected via the cross-attention layers.

Latent Input Formulation. For a given source video, we sample a clip $\mathbf{X}_{\text{clean}}$ of length L_c . The initial L_m frames serve as motion frames \mathbf{X}_{mf} to capture historical context, while the subsequent frames function as generation targets. A reference frame \mathbf{X}_{ref} is randomly sampled from outside the clip boundaries. All inputs are encoded by the 3D VAE and assembled to form the DiT input \mathbf{z}_{in} :

$$\begin{aligned} \mathbf{z}_{\text{in}} &= \mathbf{z}_{\text{noise}} \parallel \mathbf{z}_{\text{mask}} \parallel \mathbf{z}_{\text{cond}}, \quad \text{where } \mathbf{z}_{\text{mask}} = \mathbf{1}_1 \oplus \mathbf{0}_{L_c-1}, \\ \mathbf{z}_{\text{noise}} &= \mathcal{E}(\mathbf{X}_{\text{mf}}) \oplus \psi(\mathcal{E}(\mathbf{X}_{\text{clean}}), t), \quad \mathbf{z}_{\text{cond}} = \mathcal{E}(\mathbf{X}_{\text{ref}} \oplus \mathbf{0}_{L_c-1}), \end{aligned} \quad (1)$$

where \oplus denotes frame-wise concatenation and \parallel denotes channel-wise concatenation. $\mathcal{E}(\cdot)$ represents the 3D VAE encoder. The stream $\mathbf{z}_{\text{noise}}$ combines historical latents with noisy latents derived by applying the forward diffusion process $\psi(\cdot)$ to $\mathcal{E}(\mathbf{X}_{\text{clean}})$ at timestep t . The stream \mathbf{z}_{cond} injects reference guidance, while \mathbf{z}_{mask} identifies reference frames using a binary indicator. This composite input structure facilitates bidirectional interaction between historical motion context and the current generation target, allowing the model to correct accumulated errors using reference information.

2.2 Model Training

To satisfy real-time inference under strict latency constraints, we employ a two-stage training strategy. Latency-Aware Spatiotemporal Adaptation adapts the model to reduced spatial resolutions and shorter frame sequences, while Self-Correcting Bidirectional Distillation further reduces sampling steps and removes classifier-free guidance [Ho and Salimans, 2022]. This two-stage procedure enables rapid model responses while preserving high generation quality.

Stage 1: Latency-Aware Spatiotemporal Adaptation

The high computational cost of the 14B-parameter DiT backbone poses a significant challenge for real-time applications. While the original InfiniteTalk model delivers high-quality results, its inference latency on standard hardware is too high for interactive streaming. Consequently, we adapt the model to function at reduced spatial resolutions and with shorter frame sequences.

Deploying the pre-trained model directly under these constrained settings results in poor feature alignment and reduced generation quality. We address this by performing a dedicated fine-tuning phase optimized for the target resolution and frame count. During this phase, we apply a dynamic aspect-ratio bucketing strategy to organize training samples efficiently, reducing data loss from padding or cropping. This process enables the 14B model to recover fine details and maintain identity consistency, even at lower resolutions.

Stage 2: Self-Correcting Bidirectional Distillation

Multi-step sampling and classifier-free guidance create significant computational overhead. We adopt the DMD framework [Yin et al., 2024] to compress the sampling steps and eliminate the need for guidance, enabling real-time streaming.

The framework aims to minimize the distributional discrepancy between the original teacher model and the distilled student model at each time step t , using the Kullback–Leibler (KL) divergence as the optimization criterion. The resulting training objective is formulated as:

$$\nabla_{\theta} \mathcal{L}_{\text{DMD}} = -\mathbb{E}_{t, \mathbf{z}} \left[(s_{\text{real}}(\psi(G_{\theta}(z), t), t) - s_{\text{fake}}(\psi(G_{\theta}(z), t), t)) \frac{\partial G_{\theta}(\mathbf{z})}{\partial \theta} \right], \quad (2)$$

Where, $s_{\text{real}}(\cdot)$ is frozen to model the teacher distribution, while $s_{\text{fake}}(\cdot)$ is trainable and tracks the evolving student distribution. The student generator $G_{\theta}(\cdot)$ produces samples via few-step inference without classifier-free guidance. All components are initialized from the Stage-1 SFT model.

Standard DMD does not address error accumulation or identity drift in long-form videos. Inspired by Self-Forcing++ [Cui et al., 2025], we introduce Self-Correcting Bidirectional Distillation, which incorporates a multi-step retrospective self-correction mechanism to explicitly simulate error propagation during long-horizon generation. Specifically, the generator is required to autoregressively synthesize K consecutive chunks, where each chunk is conditioned on the previously generated motion frame rather than the ground truth.

To balance computational efficiency and training stability, we further propose a **Stochastic Truncation Strategy**. Instead of synthesizing all K chunks, we randomly sample a smaller value $k < K$ and generate only the first k chunks. During backpropagation, a denoising step t' is randomly sampled from the T reduced sampling steps, and gradients are retained *only* for the t' -th denoising step of the k -th chunk, while all other steps are detached from the computational graph. This stochastic truncation yields a memory-efficient yet unbiased approximation of the full training objective, which can be expressed as:

$$\nabla_{\theta} \mathcal{L} = \mathbb{E}_{k \sim \mathcal{U}(1, K), t' \sim \mathcal{U}(1, T)} \left[\nabla_{\theta} \mathcal{L}_{\text{DMD}} \left(G_{\theta}^{(k, t')}(\mathbf{z}) \right) \right], \quad (3)$$

where $G_{\theta}^{(k, t')}(\mathbf{z})$ denotes the model output at the t' -th denoising step of the k -th chunk, and all preceding chunks and denoising steps are detached from the computational graph during backpropagation.

Following this two-stage training strategy, SoulX-FlashTalk achieves state-of-the-art performance in both inference speed and generation quality compared to existing audio-driven video generation models.

2.3 Real-time Inference Acceleration

Purely optimizing training and inference in isolation is insufficient to fully satisfy stringent low-latency requirements. To achieve sub-second latency with the 14B-parameter model, we implement a full-stack acceleration suite specifically designed for 8-H800 node.

The core computational bottleneck lies within the DiT’s massive attention operations. To dismantle this barrier, we deploy Hybrid Sequence Parallelism powered by xDiT. By synergizing Ulysses and Ring Attention mechanisms, we effectively distribute the attention workload, yielding a substantial $5\times$ speedup in single-step inference compared to standard implementations. Furthermore, we optimize the DiT at the kernel level by adopting FlashAttention3, which is specifically designed to leverage the NVIDIA Hopper architecture, including its asynchronous execution pipeline. This enables improved overlap between data movement and computation, resulting in an additional 20% reduction in attention latency compared to FlashAttention2.

As DiT inference becomes sufficiently accelerated, the computational overhead of the high-resolution VAE decoder emerges as the dominant latency factor. To address this paradigm shift, we introduce 3D VAE Parallelism to mitigate the decoding burden. By employing slicing-based strategies to distribute spatial decoding workloads across GPUs, we achieve an approximate $5\times$ acceleration in VAE processing, ensuring that it does not become a pipeline bottleneck.

Finally, to eliminate overhead from the Python runtime and fragmented kernel execution, the entire inference pipeline is unified and optimized via `torch.compile`. This enables aggressive graph-level fusion and memory optimization, maximizing the hardware utilization limits of the H800 node.

2.4 Architectural Analysis: Why Bidirectional?

Although autoregressive models dominate streaming video generation, their inherent unidirectional dependency fundamentally constrains the modeling of global temporal structure. Under this paradigm, models primarily condition on historical frames and typically avoid strict frame-by-frame synthesis. Instead, generation is performed in minimal chunks to improve local consistency, where bidirectional attention is applied within each chunk, while unidirectional dependencies are enforced across chunks. However, this compromise remains insufficient to prevent temporal inconsistency, error accumulation, and identity drift, particularly in long-horizon generation.

We argue that, for the target task, incorporating long histories is not the primary bottleneck. Rather, effectively suppressing temporal drift and accumulated errors is of greater importance. Motivated by this observation, we fully preserve the bidirectional attention mechanism of the original model, consistently allowing all-to-all information exchange among frames. This design enables the model to jointly leverage past and implicit future context, resulting in more accurate and coherent generation at each step, while remaining fully aligned with the teacher architecture, thereby significantly accelerating model training.

Such bidirectional modeling not only substantially improves spatio-temporal coherence within individual chunks, but also provides a more robust and high-quality fundamental unit for streaming generation, thereby effectively mitigating drift and collapse issues in long-sequence video generation as a whole.

3 Experiment

Implementation. We build our model upon the InfiniteTalk architecture, optimizing it to satisfy real-time constraints. The training pipeline begins with a lightweight Supervised Fine-Tuning (SFT) phase of 1,000 steps to adapt the model to the reduced spatial resolutions and frame counts required for streaming. The subsequent distillation phase converges within 200 steps. We adhere to the Self-Forcing training paradigm, setting learning rates to 2×10^{-6} for the Generator and 4×10^{-7} for the Fake Score Network with a 1:5 update ratio. To simulate error accumulation in long-horizon generation, the Generator synthesizes up to $K = 5$ consecutive chunks during distillation. To accommodate variable aspect ratios in real-world data, we employ a bucketing strategy across both SFT and distillation stages. All experiments utilize a cluster of 32 NVIDIA H20 GPUs with a per-GPU batch size of 1. We enable efficient training of the 14B-parameter model under these hardware constraints via Fully Sharded Data Parallel (FSDP) [Zhao et al., 2023], gradient checkpointing, and mixed-precision training.

Datasets. We source training and evaluation data from the public SpeakerVid-5M [Zhang et al., 2025] and TalkVid [Chen et al., 2025] datasets, ensuring no overlap between training and test splits. To evaluate model performance, we construct a dedicated benchmark named TalkBench. This benchmark comprises two subsets: *TalkBench-Short*, which contains 100 samples with durations under 10 seconds, and *TalkBench-Long*, which consists of 20 samples exceeding 5 minutes.

Table 1: Quantitative comparison of SoulX-FlashTalk and state-of-the-art methods on TalkBench-Short (10 s) and TalkBench-Long (> 5 min). Models marked with * support real-time inference, and \triangle denotes the LoRA version.

Dataset	Model	Metrics								
		ASE \uparrow	IQA \uparrow	Sync-C \uparrow	Sync-D \downarrow	Subject-C \uparrow	BG-C \uparrow	Motion-S \uparrow	Temporal-F \uparrow	FPS \uparrow
Short	Ditto* [Li et al., 2025]	3.10	4.37	1.04	12.58	99.80	99.23	99.75	99.86	21.80
	Echomimic-V3 [Meng et al., 2025]	<u>3.45</u>	<u>4.70</u>	0.89	12.81	98.75	95.98	99.54	99.44	0.53
	StableAvatar [Tu et al., 2025]	3.05	3.01	0.78	12.12	98.34	96.46	99.44	99.06	0.64
	OminiAvatar [Gan et al., 2025]	3.06	3.01	<u>1.32</u>	<u>11.85</u>	98.64	96.95	99.60	<u>99.66</u>	0.16
	LiveAvatar* [Huang et al., 2025a]	3.10	3.25	1.01	12.10	98.27	97.48	99.25	98.86	20.88
	Infinitetalk \triangle [Yang et al., 2025]	3.09	3.04	1.25	11.89	98.71	97.04	99.54	99.34	5.10
Long	SoulX-FlashTalk* (Ours)	3.51	4.79	1.47	11.56	<u>99.22</u>	<u>98.10</u>	<u>99.61</u>	99.52	32.00
	Ditto* [Li et al., 2025]	3.11	3.03	0.83	13.45	99.80	99.23	99.76	99.89	0.53
	StableAvatar [Tu et al., 2025]	3.11	3.02	0.70	12.73	98.38	96.42	99.42	98.99	0.64
	OminiAvatar [Gan et al., 2025]	2.92	2.82	0.99	12.80	85.42	86.59	99.61	99.57	0.16
	LiveAvatar* [Huang et al., 2025a]	3.15	3.06	0.96	12.73	98.19	97.39	99.26	98.87	<u>20.88</u>
	InfiniteTalk \triangle [Yang et al., 2025]	3.12	3.03	<u>1.51</u>	<u>12.28</u>	98.97	97.32	99.59	99.50	5.10
	SoulX-FlashTalk* (Ours)	<u>3.12</u>	<u>3.04</u>	1.61	12.25	<u>99.29</u>	<u>98.36</u>	<u>99.63</u>	<u>99.58</u>	32.00

Evaluation Metrics. We use the Q-Align visual-language model [Wu et al., 2023] for Image Quality Assessment (IQA) and Aesthetics Score Evaluation (ASE). Lip-audio synchronization is measured via Sync-C and Sync-D metrics [Chung and Zisserman, 2016]. Furthermore, we adopt VBFench [Huang et al., 2024] to evaluate temporal quality, covering Subject Consistency (Subject-C), Background Consistency (BG-C), Motion Smoothness (Motion-S), and Temporal Flickering (Temporal-F).

3.1 Performance of SoulX-FlashTalk

SoulX-FlashTalk against state-of-the-art audio-driven generation models, including Ditto [Li et al., 2025], EchoMimic-V3 [Meng et al., 2025], StableAvatar [Tu et al., 2025], OmniAvatar [Gan et al., 2025], InfiniteTalk [Yang et al., 2025], and LiveAvatar [Huang et al., 2025a].

3.1.1 Quantitative Analysis

Table. 1 compares SoulX-FlashTalk with state-of-the-art methods on the TalkBench-Short and TalkBench-Long datasets.

On the short-video benchmark, SoulX-FlashTalk achieves the highest scores in visual quality and synchronization. Specifically, it records an ASE of 3.51 and an IQA of 4.79, surpassing the previous best performer, Echomimic-V3, which scored 3.45 and 4.70 respectively. In terms of lip-sync precision, our model attains a Sync-C score of 1.47, outperforming the 1.32 score of OmniAvatar. For inference speed, the system achieves a throughput of 32 FPS on a 14B-parameter model. This exceeds the real-time requirement of 25 FPS and significantly outperforms the 20.88 FPS recorded by LiveAvatar.

Regarding temporal consistency metrics such as Subject-C and BG-C, Ditto records the highest values across both datasets, including a Subject-C of 99.80. This performance is attributed to Ditto’s generation paradigm which inpaints only the facial region while keeping the background and torso pixel-wise static. While this approach maximizes stability scores, it precludes the generation of full-body dynamics. SoulX-FlashTalk is designed to synthesize audio-driven full-body motion which naturally introduces greater pixel variance. Despite this increased complexity, it maintains a Subject-C score of 99.22, demonstrating a balance between motion expressiveness and temporal stability.

For long-form generation, we assess robustness through synchronization retention. SoulX-FlashTalk achieves a Sync-C of 1.61 and a Sync-D of 12.25. These scores are better than InfiniteTalk and LiveAvatar. Additionally, the model sustains a throughput of 32 FPS in long-duration tasks. These results confirm that the bidirectional distillation strategy effectively reduces the desynchronization and drift often found in unidirectional streaming models.



Figure 3: **Visual quality comparison on 5-second video generation.** Orange boxes highlight static hand poses in Ditto, while blue boxes highlight significant artifacts (e.g., hand distortion, over-exposure) in baselines. In contrast, SoulX-FlashTalk eliminates these artifacts, demonstrating superior structural integrity and detail fidelity.

3.1.2 Qualitative Analysis

This section presents a qualitative assessment of SoulX-FlashTalk, focusing on generation fidelity, long-term stability, and lip-sync precision.

Visual Fidelity and Detail Preservation. Figure. 3 compares the visual quality of 5-second video generations. Baseline models demonstrate significant struggles with plausible dynamics during large limb movements. Ditto fails to synthesize meaningful hand motion, with poses remaining static throughout the sequence, as highlighted in orange. EchoMimic-v3 and StableAvatar exhibit structural distortions and artifacts in hand regions, marked in blue. InfiniteTalk suffers from hand over-exposure and excessive motion blur during rapid gestures. In contrast, SoulX-FlashTalk leverages its 14B DiT architecture and bidirectional attention mechanism to eliminate these artifacts. It synthesizes clear, structurally sound hand movements with sharp textures, avoiding the issues observed in baselines. Furthermore, our method surpasses LiveAvatar in background consistency and identity fidelity.

Stability in Infinite Generation. Figure. 4 evaluates generation stability over continuous sequences extending to 1000 seconds. Baseline models, including LiveAvatar, StableAvatar, and InfiniteTalk, suffer from significant error accumulation over time. As indicated by the blue boxes, these methods exhibit severe texture blurring and loss of detail in background regions. SoulX-FlashTalk mitigates error propagation through bidirectional streaming distillation and its self-correction mechanism. As shown in the orange boxes, our model preserves consistent facial geometry and sharp background details at the 1000-second mark, verifying its robustness for infinite streaming.

Fine-grained Lip-sync Precision. Figure. 5 assesses lip-sync fidelity during specific Chinese phonetic articulations. Baseline methods struggle with complex phonemes, exhibiting structural misalignment. As highlighted by the yellow dashed boxes, during the articulation of characters such as “上” (shàng) and “突” (tū), competitors fail to match the mouth aperture and shape of the Ground Truth (GT), resulting in visible distortions. Conversely, SoulX-FlashTalk captures these fine-grained phonemic dynamics, yielding lip geometries that are rigorously aligned with the GT. This precision minimizes lip-sync drift and stiffness, ensuring visual authenticity across different languages.

3.2 Distillation Ablations

3.2.1 Impact of Multi-step Retrospective Self-Correction

We analyze how the number of generated chunks K and scheduling strategies affect long-term stability. We compare fixed chunk strategies where K equals 1, 3, or 5 against a Random Strategy that samples K from 1 to 5 during training.

Table. 2 indicates that training with a single chunk $K = 1$ yields the lowest training cost of 2.33 hours but fails to maintain long-term stability. This is evidenced by a low Sync-C score of 1.12 on long videos, confirming the issue of error accumulation. Increasing K to 3 improves stability significantly. However, further increasing K to 5 raises the training cost to 6.40 hours without delivering proportional gains in synchronization performance. The Random

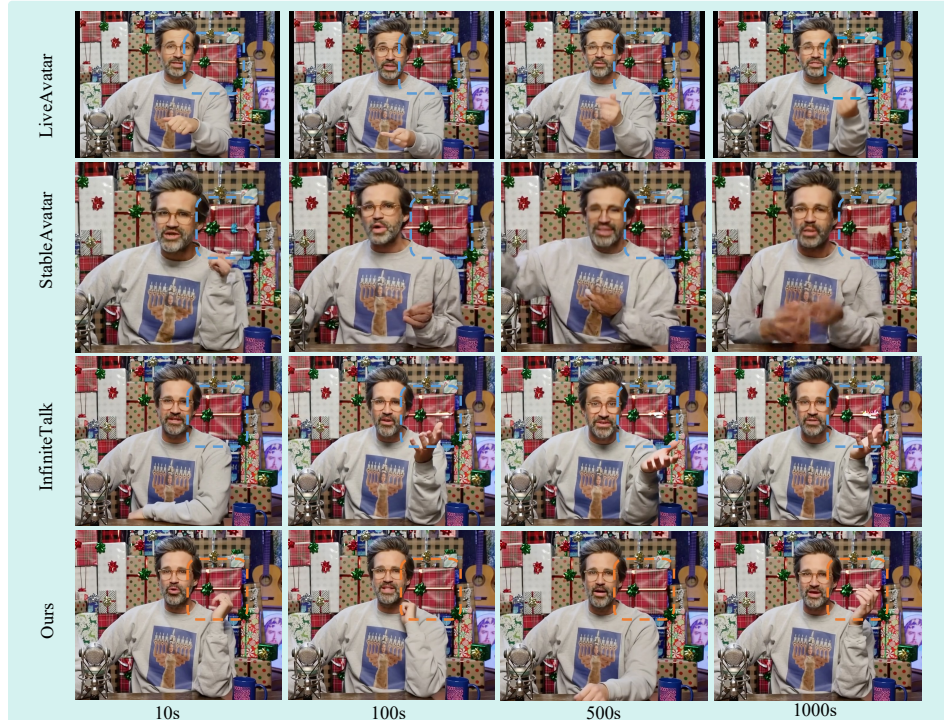


Figure 4: **Qualitative evaluation of long-term stability.** Comparison across 10s to 1000s reveals structural collapse in baselines (blue boxes) versus the sustained robustness of SoulX-FlashTalk (orange boxes), which preserves sharp details even after 1000 seconds of continuous generation.

Table 2: Ablation study on chunk generation strategies during distillation.

Strategy	ASE ↑		IQA ↑		Syn-C ↑		Sync-D ↓		Training Cost (h) ↓	
	short	long	short	long	short	long	short	long		
Fixed	$K = 1$	3.42	3.08	4.69	2.99	1.39	1.12	11.79	12.47	2.33
	$K = 3$	3.47	3.09	4.75	3.00	1.39	1.59	11.69	12.02	4.40
	$K = 5$	3.50	3.10	4.79	3.01	1.35	1.44	11.87	12.33	6.40
Random	[1, 5]	3.51	3.12	4.79	3.04	1.47	1.61	11.56	12.25	4.40

strategy achieves the best overall balance. It attains the highest Long Sync-C score of 1.61 and optimal visual quality metrics while maintaining a moderate training cost of 4.40 hours. This demonstrates that exposing the model to varying autoregressive lengths during distillation effectively improves robustness against accumulated errors.

3.2.2 Impact of Motion Latent Conditioning in DMD

We examine the conditioning of the Real Score network across three dimensions: the source of motion latents, noise injection, and loss computation. Table. 3 shows that using student-predicted motion latents yields better visual quality than using Ground Truth (GT) latents. Specifically, the Predicted strategy with noise achieves an ASE of 3.51 and an IQA of 4.79, surpassing the GT configuration which scores 3.48 and 4.77. This indicates that using predicted latents helps reduce the disparity between training and inference.

Regarding noise and loss, injecting noise into predicted latents improves performance, raising ASE from 3.46 to 3.51. Conversely, including motion latents in the loss computation lowers the ASE to 3.48. This suggests that requiring the model to reconstruct conditioning frames diverts focus from the primary denoising task. Thus, the configuration of Predicted Latents with Noise Injection and No Loss delivers the optimal results.



Figure 5: **Qualitative comparison of lip-sync precision on Chinese pronunciations.** Yellow dashed boxes indicate lip shape distortions in baseline methods for characters “上”, “突” and, “法”, whereas our method achieves high alignment with the Ground Truth (GT).

Table 3: Ablation on the conditioning of motion latents in the Real Score Network.

Motion Source	Noise Strategy		Metrics			
	Add Noise	Calc Loss	ASE \uparrow	IQA \uparrow	Sync-C \uparrow	Sync-D \downarrow
Ground Truth Latents	✗	✗	3.46	4.75	1.43	11.68
Ground Truth Latents	✓	✗	3.48	4.77	1.34	11.82
Predicted Latents	✗	✗	3.46	4.75	1.43	11.68
Predicted Latents	✓	✗	3.51	4.79	1.47	11.56
Predicted Latents	✓	✓	3.48	4.77	1.35	11.94

3.3 Inference Latency Analysis

In this section, we analyze component-wise latency on a single-node system with varying numbers of NVIDIA H800 GPUs. The experimental setup targets high-fidelity streaming at a resolution of 720×416 with 4-step denoising. Each clip comprises 33 frames, including 28 generated frames and 5 motion frames. Under this configuration, the pipeline achieves a throughput of up to 32 FPS.

The latency of the VAE and DiT is first examined to highlight the necessity of multi-GPU parallelism, as summarized in Table 4. On a single GPU, DiT inference alone incurs a latency of 1070 ms per step, while VAE inference requires 97 ms for motion frames encoding and 988 ms for generated frames decoding.

When scaling to 8 GPUs, DiT and VAE are parallelized using xDiT’s hybrid sequence parallelism and LightX2V’s slicing-based parallel strategy, respectively. Due to inter-GPU communication overhead, the acceleration is slightly sub-linear, resulting in an overall speedup of nearly 5 \times . Concretely, DiT latency is reduced from 1070 ms to 193 ms, VAE encoding from 97 ms to 21 ms, and decoding from 988 ms to 192 ms. Additional latency reductions are achieved by enabling `torch.compile`.

Table 4: Inference latency breakdown across varying GPU counts (Unit: ms).

GPUs	VAE		DiT	
	Encode	Decode	w/o torch.compile	w/ torch.compile
1	97	988	1070	800
2	69	690	620	490
4	39	350	313	261
8	21	192	193	154
<i>-w/ torch.compile</i>	14	187		

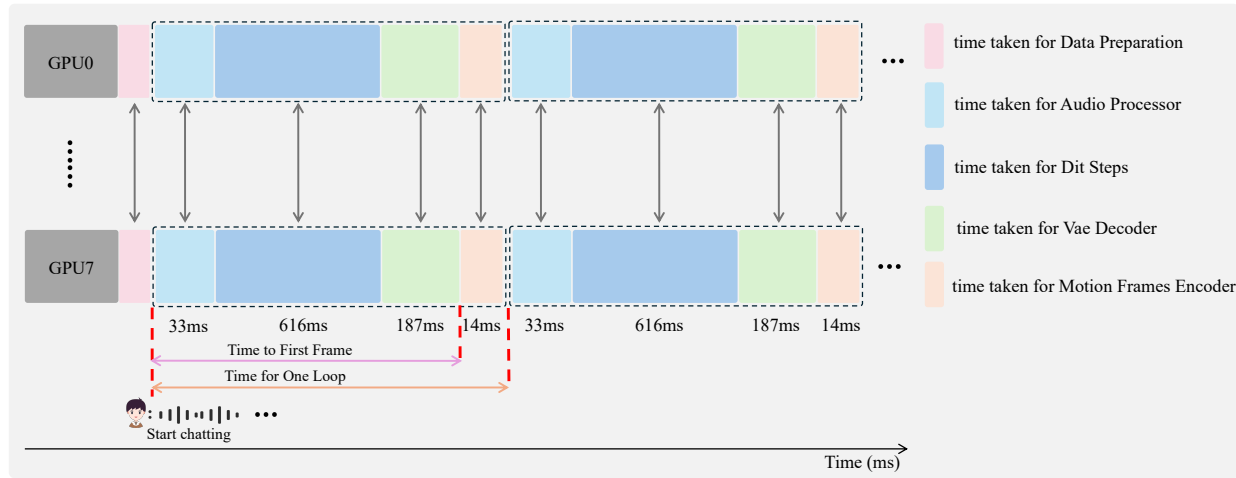


Figure 6: Detailed inference latency breakdown on 8 NVIDIA H800 GPUs.

Building upon the core component optimizations, we report the end-to-end pipeline latency on an $8 \times$ H800 GPU cluster in Figure. 6. During the steady-state generation loop, the total latency per cycle is 876 ms, of which audio processing takes 33 ms, the core 4-step DiT denoising accounts for 616 ms, frame decoding consumes 187 ms, and motion-frame encoding requires 14 ms. The remaining latency is attributed to miscellaneous overheads. By achieving sub-second end-to-end latency, the proposed pipeline meets the stringent throughput requirements of real-time streaming.

4 Conclusion and Future Work

We presented SoulX-FlashTalk, a framework designed to meet real-time requirements while maintaining high-quality video synthesis. Integrating Bidirectional Streaming Distillation with a Multi-step Self-Correction mechanism allows our 14B-parameter DiT model to sustain stable, infinite-length streaming on an $8 \times$ H800 cluster. Our approach also simplifies training. We demonstrate that complex multi-stage pre-training is not required. A brief SFT phase followed by distribution matching distillation suffices to achieve state-of-the-art performance. We are open-sourcing this solution to serve as a practical baseline for the community.

Future work will prioritize model efficiency over system scaling. We intend to explore pruning, quantization, and optimized attention mechanisms. The objective is to deploy these models on consumer-grade hardware, eliminating the dependency on expensive computing clusters.

5 Ethics Statement

This research aims to advance digital human synthesis for beneficial applications. We confirm that all datasets utilized in this study are derived from publicly accessible academic repositories. The visual demonstrations presented in this report are fully synthetic and do not contain the Personally Identifiable Information (PII) of private individuals.

We acknowledge the dual-use nature of high-fidelity video generation technology and the potential risks associated with its misuse, such as the creation of deepfakes or the spread of misinformation. We firmly condemn any malicious application of this technology and advocate for the principles of Responsible AI. To mitigate these risks, we support the development of robust forgery detection algorithms and the implementation of invisible watermarking mechanisms to ensure content transparency and traceability. We remain committed to adhering to ethical guidelines and ensuring that our contributions promote the safe and positive evolution of the field.

6 Project Contributions

All contributors are listed in no particular order.

- **Project Sponsor:** Ming Tao, Shunshun Yin
- **Project Leader:** Siyuan Liu
- **Algorithm:** Le Shen, Qian Qiao, Tan Yu
- **Deployment & Acceleration:** Ke Zhou, Tianhang Yu, Yu Zhan
- **Data & Evaluation:** Tan Yu, Tianhang Yu, Dingcheng Zhen

References

- William Peebles and Saining Xie. Scalable diffusion models with transformers. In *Proceedings of the IEEE/CVF international conference on computer vision*, pages 4195–4205, 2023.
- Xin Gao, Li Hu, Siqi Hu, Mingyang Huang, Chaonan Ji, Dechao Meng, Jinwei Qi, Penchong Qiao, Zhen Shen, Yafei Song, et al. Wan-s2v: Audio-driven cinematic video generation. *arXiv preprint arXiv:2508.18621*, 2025.
- Zhizhou Zhong, Yicheng Ji, Zhe Kong, Yiyi Liu, Jiarui Wang, Jiasun Feng, Lupeng Liu, Xiangyi Wang, Yanjia Li, Yuqing She, et al. Anytalker: Scaling multi-person talking video generation with interactivity refinement. *arXiv preprint arXiv:2511.23475*, 2025.
- Jianzhu Guo, Dingyun Zhang, Xiaoqiang Liu, Zhizhou Zhong, Yuan Zhang, Pengfei Wan, and Di Zhang. Liveportrait: Efficient portrait animation with stitching and retargeting control. *arXiv preprint arXiv:2407.03168*, 2024.
- Shaoshu Yang, Zhe Kong, Feng Gao, Meng Cheng, Xiangyu Liu, Yong Zhang, Zhuoliang Kang, Wenhan Luo, Xunliang Cai, Ran He, et al. Infinitetalk: Audio-driven video generation for sparse-frame video dubbing. *arXiv preprint arXiv:2508.14033*, 2025.
- Yubo Huang, Hailong Guo, Fangtai Wu, Shifeng Zhang, Shijie Huang, Qijun Gan, Lin Liu, Sirui Zhao, Enhong Chen, Jiaming Liu, et al. Live avatar: Streaming real-time audio-driven avatar generation with infinite length. *arXiv preprint arXiv:2512.04677*, 2025a.
- Tianwei Yin, Michaël Gharbi, Richard Zhang, Eli Shechtman, Fredo Durand, William T Freeman, and Taesung Park. One-step diffusion with distribution matching distillation. In *Proceedings of the IEEE/CVF conference on computer vision and pattern recognition*, pages 6613–6623, 2024.
- Xun Huang, Zhengqi Li, Guande He, Mingyuan Zhou, and Eli Shechtman. Self forcing: Bridging the train-test gap in autoregressive video diffusion. *arXiv preprint arXiv:2506.08009*, 2025b.
- Justin Cui, Jie Wu, Ming Li, Tao Yang, Xiaojie Li, Rui Wang, Andrew Bai, Yuanhao Ban, and Cho-Jui Hsieh. Self-forcing++: Towards minute-scale high-quality video generation. *arXiv preprint arXiv:2510.02283*, 2025.
- Sam Ade Jacobs, Masahiro Tanaka, Chengming Zhang, Minjia Zhang, Shuaiwen Leon Song, Samyam Rajbhandari, and Yuxiong He. Deepspeed ulysses: System optimizations for enabling training of extreme long sequence transformer models. *arXiv preprint arXiv:2309.14509*, 2023.
- Hao Liu, Matei Zaharia, and Pieter Abbeel. Ring attention with blockwise transformers for near-infinite context. *arXiv preprint arXiv:2310.01889*, 2023.
- LightX2V Contributors. Lightx2v: Light video generation inference framework. <https://github.com/ModelTC/lightx2v>, 2025.
- Jay Shah, Ganesh Bikshandi, Ying Zhang, Vijay Thakkar, Pradeep Ramani, and Tri Dao. Flashattention-3: Fast and accurate attention with asynchrony and low-precision. *Advances in Neural Information Processing Systems*, 37: 68658–68685, 2024.
- Team Wan, Ang Wang, Baole Ai, Bin Wen, Chaojie Mao, Chen-Wei Xie, Di Chen, Fei Yu, Haiming Zhao, Jianxiao Yang, et al. Wan: Open and advanced large-scale video generative models. *arXiv preprint arXiv:2503.20314*, 2025.

- Alexei Baevski, Yuhao Zhou, Abdelrahman Mohamed, and Michael Auli. wav2vec 2.0: A framework for self-supervised learning of speech representations. *Advances in neural information processing systems*, 33:12449–12460, 2020.
- Alec Radford, Jong Wook Kim, Chris Hallacy, Aditya Ramesh, Gabriel Goh, Sandhini Agarwal, Girish Sastry, Amanda Askell, Pamela Mishkin, Jack Clark, Gretchen Krueger, and Ilya Sutskever. Learning transferable visual models from natural language supervision. In Marina Meila and Tong Zhang, editors, *Proceedings of the 38th International Conference on Machine Learning, ICML 2021, 18-24 July 2021, Virtual Event*, volume 139 of *Proceedings of Machine Learning Research*, pages 8748–8763. PMLR, 2021. URL <http://proceedings.mlr.press/v139/radford21a.html>.
- Colin Raffel, Noam Shazeer, Adam Roberts, Katherine Lee, Sharan Narang, Michael Matena, Yanqi Zhou, Wei Li, and Peter J. Liu. Exploring the limits of transfer learning with a unified text-to-text transformer. *J. Mach. Learn. Res.*, 21:140:1–140:67, 2020. URL <https://jmlr.org/papers/v21/20-074.html>.
- Jonathan Ho and Tim Salimans. Classifier-free diffusion guidance. *arXiv preprint arXiv:2207.12598*, 2022.
- Yanli Zhao, Andrew Gu, Rohan Varma, Liang Luo, Chien-Chin Huang, Min Xu, Less Wright, Hamid Shojanazeri, Myle Ott, Sam Shleifer, et al. Pytorch fsdp: experiences on scaling fully sharded data parallel. *arXiv preprint arXiv:2304.11277*, 2023.
- Youliang Zhang, Zhaoyang Li, Duomin Wang, Jiahe Zhang, Deyu Zhou, Zixin Yin, Xili Dai, Gang Yu, and Xiu Li. Speakervid-5m: A large-scale high-quality dataset for audio-visual dyadic interactive human generation. *arXiv preprint arXiv:2507.09862*, 2025.
- Shunian Chen, Hejin Huang, Yixin Liu, Zihan Ye, Pengcheng Chen, Chenghao Zhu, Michael Guan, Rongsheng Wang, Junying Chen, Guanbin Li, Ser-Nam Lim, Harry Yang, and Benyou Wang. Talkvid: A large-scale diversified dataset for audio-driven talking head synthesis, 2025. URL <https://arxiv.org/abs/2508.13618>.
- Haoning Wu, Zicheng Zhang, Weixia Zhang, Chaofeng Chen, Liang Liao, Chunyi Li, Yixuan Gao, Annan Wang, Erli Zhang, Wenxiu Sun, et al. Q-align: Teaching lmms for visual scoring via discrete text-defined levels. *arXiv preprint arXiv:2312.17090*, 2023.
- Joon Son Chung and Andrew Zisserman. Out of time: automated lip sync in the wild. In *Asian conference on computer vision*, pages 251–263. Springer, 2016.
- Ziqi Huang, Yinan He, Jiashuo Yu, Fan Zhang, Chenyang Si, Yuming Jiang, Yuanhan Zhang, Tianxing Wu, Qingyang Jin, Nattapol Chanpaisit, Yaohui Wang, Xinyuan Chen, Limin Wang, Dahua Lin, Yu Qiao, and Ziwei Liu. VBench: Comprehensive benchmark suite for video generative models. In *Proceedings of the IEEE/CVF Conference on Computer Vision and Pattern Recognition*, 2024.
- Tianqi Li, Ruobing Zheng, Minghui Yang, Jingdong Chen, and Ming Yang. Ditto: Motion-space diffusion for controllable realtime talking head synthesis. In *Proceedings of the 33rd ACM International Conference on Multimedia*, pages 9704–9713, 2025.
- Rang Meng, Yan Wang, Weipeng Wu, Ruobing Zheng, Yuming Li, and Chenguang Ma. Echomimicv3: 1.3 b parameters are all you need for unified multi-modal and multi-task human animation. *arXiv preprint arXiv:2507.03905*, 2025.
- Shuyuan Tu, Yueming Pan, Yimeng Huang, Xintong Han, Zhen Xing, Qi Dai, Chong Luo, Zuxuan Wu, and Yu-Gang Jiang. Stableavatar: Infinite-length audio-driven avatar video generation. *arXiv preprint arXiv:2508.08248*, 2025.
- Qijun Gan, Ruizi Yang, Jianke Zhu, Shaofei Xue, and Steven Hoi. Omniaavatar: Efficient audio-driven avatar video generation with adaptive body animation. *arXiv preprint arXiv:2506.18866*, 2025.